J Fluoresc (2013) 23:311–321
DOI 10.1007/s10895-012-1149-7

ORIGINAL PAPER

Mechanistic Insights into the Inhibition of Endo-β 1,4 Xyloglucan Hydrolase by a Classical Aspartic Protease Inhibitor

Vishnu Menon · Mala Rao

Received: 3 July 2012 / Accepted: 20 November 2012 / Published online: 5 December 2012

Abstract This is the first report of inactivation of xyloglucanase from *Thermomonospora* sp by pepstatin A, a specific inhibitor towards aspartic proteases. The steady state kinetics revealed a reversible, competitive, two-step inhibition mechanism with IC_{50} and K_i values of 3.5±0.5 μM and 1.25±0.5 μM respectively. The rate constants determined for the isomerization of EI to EI* and the dissociation of EI* were 14.5±1.5×$10^{-5}s^{-1}$ and 2.85±1.2×$10^{-8}s^{-1}$ respectively, whereas the overall inhibition constant K_i^* was 27±1 nM. The conformational changes induced upon inhibitor binding to xyloglucanase were monitored by fluorescence analysis and the rate constants derived were in agreement with the kinetic data. The abolished isoindole fluorescence of o-phthalaldehyde (OPTA)-labeled xyloglucanase and far UV analysis suggested that pepstatin binds to the active site of the enzyme. Our results revealed that the inactivation of xyloglucanase is due to the interference in the electronic microenvironment and disruption of the hydrogen-bonding network between the essential histidine and other residues involved in catalysis.

Keywords Endo-β 1,4 xyloglucan hydrolase · Pepstatin · Enzyme kinetics · Slow-tight binding · Inactivation mechanism

Introduction

The vital functions of glycosidases in living systems are revealed by modifying or blocking biological processes by specific glycosidase inhibitors. Xyloglucanase or endo-β (1,4) xyloglucan hydrolase belong to the inverting and retaining glycoside hydrolyases which constitute 113 protein families responsible for the hydrolysis and/or transglycosylation of glycosidic bonds [1]. Xyloglucanases (3.2.1.151) represent a class of polysaccharide degrading enzymes which can attack the backbone also at substituted glucose residues [2]. The xyloglucan and the enzymes responsible for its modification and degradation are finding increasing prominence, reflecting the drive for diverse biotechnological applications [3–5]. Specific inhibitors are important to gain insight into the details of the hydrolytic mechanism of xyloglucanases. They can act as mechanistic and structural probes and can also establish the structures of active centers [6].

There are only few reports of naturally occurring proteinaceous inhibitors of xyloglucanase from tomato, tobacco, soybean, potato [7–11]; however there is only one reports of a low molecular weight peptidic inhibitor from microorganism (manuscript communicated). Low-molecular weight inhibitors released from microbial cells are different from macromolecular endogenous inhibitors. The low molecular weight inhibitors usually do not have functional roles in its cell, whereas the macromolecular endogenous inhibitors exhibit some functions in the cells. Therefore, much effort needs to be focused on the design of efficient and specific inhibitors of xyloglucanase for many potential applications such as prospective biocontrol agents. Pepstatin is a naturally occurring low molecular weight potent inhibitor specific for aspartic proteases [12]. The unusual potency of pepstatin toward aspartic proteases has been widely exploited as a research tool for unraveling the mechanism of this group of enzymes, its biological functions, and in affinity chromatography [13]. It also has been tested as a therapeutic agent for experimental control of gastric ulcer, carrageenin edema, hypertension, and infectious diseases

V. Menon · M. Rao (✉)
Division of Biochemical Sciences, National Chemical Laboratory, Pune 411 008, India
e-mail: mb.rao@ncl.res.in

M. Rao
e-mail: raomala04@gmail.com

like human immunodeficiency virus [14, 15]. There is only one report of pepstatin A inhibiting a xylanase [16]. To our knowledge there are no reports of inhibition on xyloglucanase by pepstatin A.

The present paper envisages the slow-tight binding inhibition of xyloglucanase from a *Thermomonospora* sp by a specific aspartic protease inhibitor, pepstatin A. The steady state kinetics revealed a two-step inhibition mechanism, and the conformational modes observed during the binding of inhibitor to the enzyme were conveniently monitored by fluorescence analysis. The mechanism of inactivation of xyloglucanase by pepstatin A was delineated by monitoring the isoindole fluorescence of the *o*-phthalaldehyde (OPTA)-labeled enzyme and far UV analysis.

Materials and Methods

Materials

Xyloglucan from tamarind seeds was a kind gift from Dr Barry McCleary, Megazyme International Ireland Ltd, Ireland. Tamarind kernel powder (TKP) was kindly provided by Mr A Agarwal, Herbex International, India. Pepstatin A, QAE Sephadex, dinitrosalicylic acid, OPTA (o-phthalaldehyde) were from Sigma-Aldrich, USA. Bio-Gel P-100 was from Bio-Rad laboratories, CA. All other chemicals used were of analytical grade.

Purification of Xyloglucanase

Thermomonspora sp was grown at 50 °C for 120 h in modified Reese medium supplemented with tamarind kernel powder and cellulose powder for the production of xyloglucanase. The enzyme was purified to homogeneity from the extracellular culture filtrate by ammonium sulphate precipitation (0–90 %), QAE-Sephadex ion exchange chromatography and Bio-Gel P-100 gel filtration chromatography [17].

Xyloglucanase Assay and Initial Kinetic Analysis

Xyloglucanase activity was measured by incubating 1 ml of assay mixture containing 0.5 ml of 5 mg/ml of tamarind xyloglucan and 0.5 ml of suitably diluted enzyme in 50 mM phosphate buffer (pH 7) for 30 min at 50 °C [4]. Enzyme and reagent blanks were also simultaneously incubated with test samples. The reducing sugar formed was estimated by dinitrosalicylic acid [18]. One unit of enzyme activity is defined as the amount of enzyme required to liberate 0.5 mg of reducing sugar per minute under assay conditions. Protein concentration was determined according to the method of Lowry [19], using bovine serum albumin as standard.

For initial kinetic analysis, the kinetic parameters for the substrate hydrolysis were determined by measuring the initial rate of enzymatic activity. The inhibition constant (K_i) was determined by Dixon method [20] and also by the Lineweaver-Burk's equation. For the Lineweaver-Burk's analysis xyloglucanase (2 μM) was incubated with the inhibitor at (0.5 μM) and (1 μM) and assayed at increased concentration of xyloglucan (1–10 mg/ml) at 50 °C for 30 min. The reciprocals of substrate hydrolysis ($1/v$) for each inhibitor concentration were plotted against the reciprocals of the substrate concentrations, and the K_i was determined by fitting the resulting data. In Dixon's method, xyloglucanolytic activity of xyloglucanase (2 μM) was measured in the presence of 5 and 10 mg/ml of xyloglucan, at concentrations of pepstatin ranging from 0 to 7 μM at 50 °C for 30 min. The reciprocals of substrate hydrolysis ($1/v$) were plotted against the inhibitor concentration and the K_i was determined by fitting the data using Microcal Origin 8E. For progress curve analysis, assays were carried out in a 1 ml reaction mixture containing enzyme, substrate, and inhibitor at various concentrations. The reaction mixture contained xyloglucanase (50 nM) in sodium phosphate buffer, 0.05 M, pH 6.0, and varying concentrations of pepstatin A (0.3 to 3 μM) and xyloglucan (10 mg/ml). Reaction was initiated by the addition of xyloglucanases at 50 °C and the release of products were quantified at different time intervals by estimating the reducing sugar at 540 nm. In each slow binding inhibition experiment, five to six assays were performed with appropriate blanks. For the kinetic analysis and rate constant determinations, the assays were carried out in triplicate and the average value was considered throughout. Further details of the experiments are given in the respective figure legends.

Evaluation of kinetic parameters—Initial rate studies for reversible; competitive inhibition was analyzed according to Eq. 1,

$$v = \frac{V_{\max} S}{K_m(1 + I/K_i) + S} \tag{1}$$

where K_m is the Michaelis constant, V_{max} is the maximal catalytic rate at saturating substrate concentration S, $K_i=(k_4/k_3)$ is the dissociation constant for the first reversible enzyme-inhibitor complex, and I is the inhibitor concentration [21]. The progress curves for the interactions between pepstatin A and xyloglucanase were analyzed using Eq. 2,

$$[P] = v_s t + \frac{v_0 - v_s}{k}\left(1 - e^{-kt}\right) \tag{2}$$

where (P) is the product concentration at any time t, v_0 and v_s are the initial and final steady-state rates, respectively, and k is the apparent first-order rate constant for the establishment of the final steady-state equilibrium. As a prerequisite for tight binding inhibitors, corrections have been made for

the reduction in the inhibitor concentration that occurs on formation of the enzyme-inhibitor (EI) complex. This is because, in the case of tight binding inhibition, the concentration of EI is not negligible in comparison to the inhibitor concentration and the free inhibitor concentration is not equal to the added concentration of the inhibitor. The corrections of the variation of the steady-state velocity with the inhibitor concentrations were made according to Eqs. 3 and 4 as described by Morrison and Walsh [22],

$$\upsilon_s = \frac{k_7 SQ}{2(K_m + S)} \tag{3}$$

$$Q = \left[\left(K_i^{'} + I_t - E_t\right) + 4K_i^{'}E_t\right]^{1/2} - \left(K_i^{'} + I_t - E_t\right) \tag{4}$$

where $K_i^{'} = K_i^{*}(1 + S/K_m)$, k_7 is the rate constant for the product formation and I_t and E_t stands for total inhibitor and enzyme concentration, respectively.

The relationship between the rate constant of enzymatic reaction k, and the kinetic constants for the association and dissociation of the enzyme and inhibitor was determined as per Eq. 5,

$$k = k_6 + k_5\left(\frac{I/K_i}{1 + (S/K_m) + (I/K_i)}\right) \tag{5}$$

The progress curves were analyzed by Eqs. 2 and 5 using nonlinear least-square parameter minimization to determine the best-fit values with the corrections for the tight binding inhibition. The overall inhibition constant is determined as given by Eq. 6,

$$K_i^{*} = \frac{[E][\mathrm{I}]}{[EI] + [EI*]} = K_i\left(\frac{k_6}{k_5 + k_6}\right) \tag{6}$$

For the time-dependent inhibition, there exists a time range in the progress curves wherein formation of EI* is small. Within this time range, it is possible to directly measure the effect of the inhibitor on v_0, i.e. to measure K_i directly. Values for K_i were obtained from Dixon analysis at a constant substrate concentration as described in Eq. 7,

$$\frac{1}{\upsilon} = \frac{1}{V_{\max}} + \frac{K_m}{V_{\max} S}(1 + I/K_i) \tag{7}$$

The rate constant k_6 for the dissociation of the second enzyme inhibitor complex was measured directly from the time-dependent inhibition. Concentrated xyloglucanase and pepstatin A were incubated in a reaction mixture to reach equilibrium followed by large dilutions in assay mixtures containing near-saturating substrate. Xyloglucanase (2 mM) was preincubated with equimolar concentrations of pepstatin A for 120 min in sodium phosphate buffer, 0.05 M, pH 6.0. 5 μl of the preincubated sample was removed and diluted 5000-fold in the same buffer and assayed at 50 °C using xyloglucanase at (100 mg/ml) at different time intervals.

Fluorescence Analysis of Enzyme-Pepstatin Interactions

Fluorescence measurements were performed on a Cary Varian Eclipse fluorescence spectrophotometer connected to a Cary Varian temperature controller. Protein fluorescence was excited at 295 nm, and the emission was recorded from 300 to 500 nm at 25 °C. The slit widths on both the excitation and emission were set at 5 nm, and the spectra were obtained at 1 nm/min. Fluorescence data were corrected by running control samples of buffer and smoothed. For inhibitor binding studies, xyloglucanase (2 μM) was dissolved in 0.05 N HCl. Titration of the enzyme with the inhibitor was performed by the addition of different concentrations of inhibitor. The magnitude of the rapid fluorescence decrease (F_0-F) occurring at each inhibitor concentration was computer fitted to the equation $(F_0 - F) = F_{max}/\{1 + (K_i/[I])\}$ to determine the calculated value of K_i and ΔF_{max}. The first-order rate constants for the slow loss of fluorescence K_{obs}, at each inhibitor concentration [I] were calculated by computer fitting of the remaining data, starting 1 s after inhibitor addition, to the equation $K_{obs} = k_5[I]/(K_i + [I])$ for the determination of k_5 under the assumption that, for a tight-binding inhibitor, k_6 can be considered negligible at the onset of the slow loss of fluorescence [21]. Time courses of the protein fluorescence following the addition of inhibitor were measured for up to 5 min with excitation and emission wavelengths fixed at 295 and 342 nm, respectively. Data points were collected at 1.0 s intervals during time courses. Corrections for the inner filter effect were performed as described by the formula [23]. F_c=F antilog $[(A_{ex} + A_{em})/2]$, where F_c and F are the corrected and measured fluorescence intensities, respectively, and A_{ex} and A_{em} are the solution absorbance at the excitation and emission wavelengths, respectively. Background buffer spectra were subtracted to remove the contribution from Raman scattering.

Effect of Pepstatin on the Isoindole Fluorescence of OPTA-Labeled Xyloglucanase

OPTA solution was prepared in methanol for each experiment. The modification was carried out by incubating xyloglucanase (2 μM) in 1 ml of 0.05 M sodium phosphate buffer, pH 6, with 50 μM OPTA at 25 °C. Methanol had no effect on the activity of the enzyme and was always less than 2 % (*v*/*v*). The formation of xyloglucanase-isoindole derivative was followed spectrofluorometrically by monitoring the increase in fluorescence with the excitation wavelength fixed at 330 nm. To monitor the effect of inhibitor on the isoindole fluorescence of xyloglucanase, the enzyme was preincubated with inhibitor (2 μM) for 15 min, and

then OPTA was added and the formation of isoindole derivative was monitored as described above.

Secondary Structural Analysis of Xyloglucanase-Pepstatin Complexes

CD spectra were recorded in a Jasco-J715 spectropolarimeter at ambient temperature using a cell of 1-mm path length. Replicate scans were obtained at 0.1-nm resolution, 0.1-nm bandwidth, and a scan speed of 50 nm/min. Spectra were averages of six scans with the base line subtracted spanning from 280 to 200 nm in 0.1-nm increments. The CD spectrum of xyloglucanase (50 nM) was recorded in 0.05 M phosphate buffer, pH 6 in the absence/presence of xyloglucan (1 μg/ml) (experiments were performed at 4 °C to avoid the hydrolysis of substrate by enzyme) or pepstatin A (5 and 10 μM).

Results

Kinetic Analysis of the Inhibition of Xyloglucanase

The aspartic protease inhibitor (pepstatin A) is well documented for its inhibitory activity toward pepsin, renin, cathepsin D, and human immunodeficiency virus 1 protease [24]. Pepstatin A was found to inhibit xyloglucanase purified from alkalothermophilic *Thermomonospora* sp. Initial kinetic assessments revealed that pepstatin A was a competitive inhibitor of xyloglucanase with an IC_{50} value of 3.5± 0.5 μM (Fig. 1a). In the presence of pepstatin A, the steady-state rate of xyloglucanolytic activity exhibited a time-dependent decrease as a function of the inhibitor concentration. Examination of the progress curves revealed a time range where the initial rate of reaction did not deviate from linearity (Fig. 1b), and the conversion of EI to EI* was minimal. For a low concentration of pepstatin A this time range was 10 min, within which classical competitive inhibition experiments was used to determine the K_i values (Eq. 5). The value of the inhibition rate constant K_i, associated with the formation of the reversible enzyme-inhibitor complex (*EI*) determined from the fits of data to the reciprocal equation, was 1.25±0.5 μM (Fig. 2a), which was corroborated by the Dixon method (Fig. 2b). The apparent rate constant k, derived from the progress curves when plotted versus the inhibitor concentration, followed a hyperbolic function (Fig. 3a), revealing that a fast equilibrium precedes the formation of the final slow dissociating enzyme-inhibitor complex (*EI**), indicating a two-step, slow-tight inhibition mechanism (Scheme 1). Indeed, the data could be fitted to Eq. 5 by non-linear regression analysis, which yielded the best estimate of the overall inhibition constant K_i^* of 27.0±1 nM.

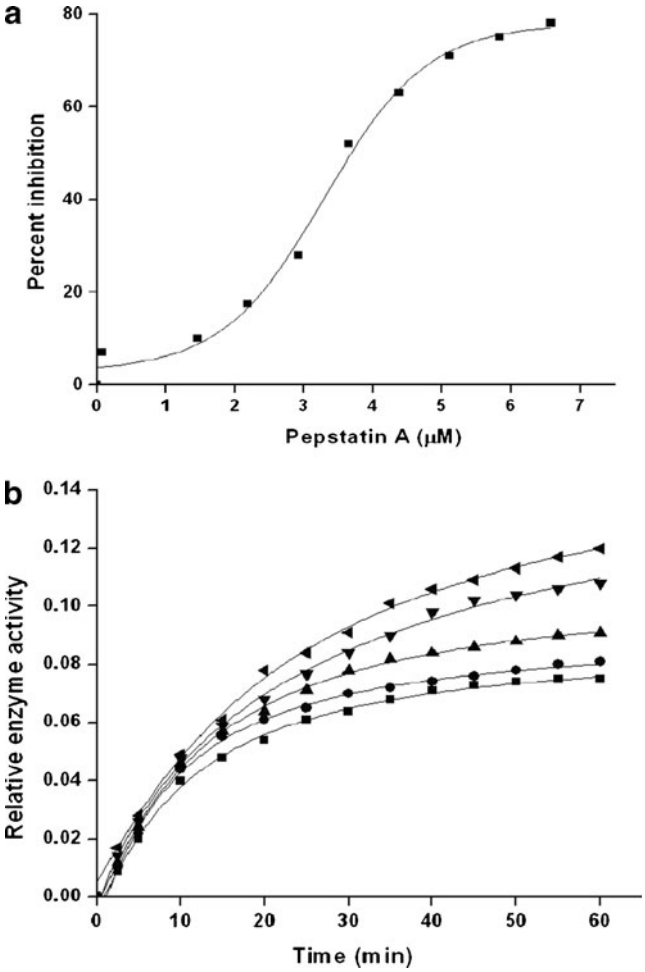

Fig. 1 **a** Inhibition of xyloglucanase by pepstatin A. The xyloglucanolytic activity of the purified enzyme (2 μM) was determined in the presence of increasing concentrations of pepstatin A. The percent inhibition of the xyloglucanase activity was calculated from the residual enzymatic activity. The sigmoidal curve indicates the best fit for the percent inhibition data (average of triplicates) obtained, and the IC_{50} value was calculated from the graph. **b** Time course of inhibition of xyloglucanase by pepstatin A. The reaction mixture contained xyloglucanase (50 nM) in sodium-phosphate buffer, 0.05 M, pH 7.0, and varying concentrations of pepstatin A and xyloglucan (10 mg/ml). Reaction was initiated by the addition of xyloglucanase at 50 °C. The points represent the hydrolysis of substrate as a function of time, and the lines indicate the best fits of data obtained from Eqs. 2 and 5, with the corrections made as per Eqs. 3 and 4. Concentrations of pepstatin A were 0.37 μM (*filled left-pointing pointer*), 0.75 μM (*filled down-pointing triangle*), 1.1 μM (*filled up-pointing triangle*), 1.5 μM (*filled circle*)**, and 3.2 μM (***filled square***)**

In an alternative method, the rate constant k_6, for the conversion of *EI** to *EI*, was determined by pre-incubating high concentrations of enzyme and inhibitor for sufficient time to allow the system to reach equilibrium. Dilution of the enzyme inhibitor complex into a relatively large volume of assay mixture containing saturating substrate concentration causes dissociation of the enzyme-inhibitor complex and, thus, regeneration of enzymatic activity. Under these

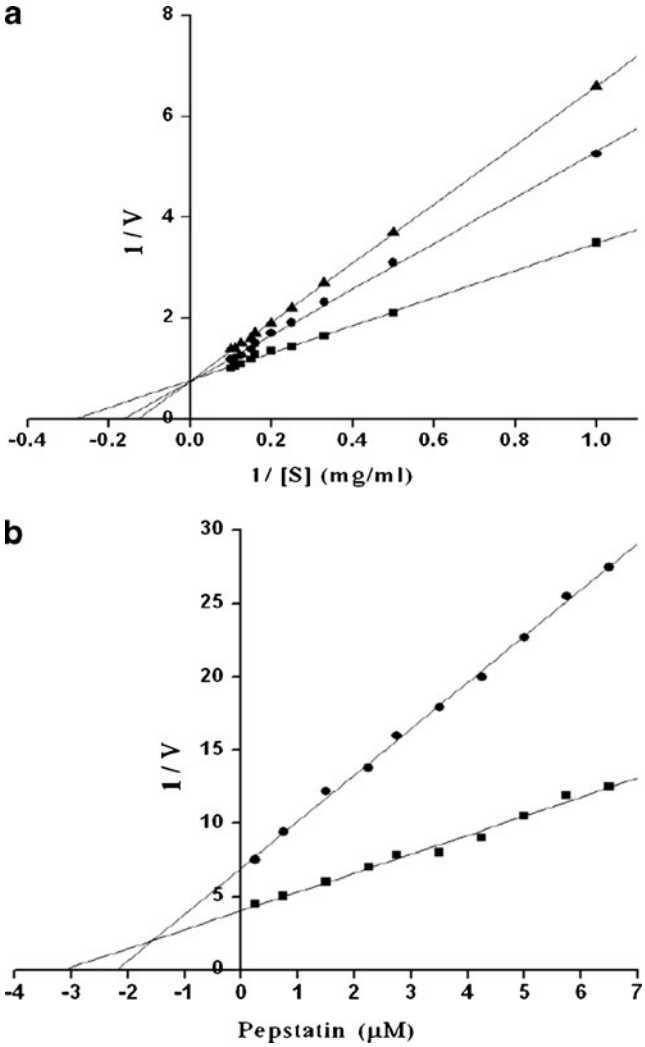

Fig. 2 Initial rate of enzymatic reaction of xyloglucanase in the presence of pepstatin A. **a** xyloglucanase activity was estimated using xyloglucan in sodium-phosphate buffer, 0.05 M, pH 7.0, and the reducing sugar was determined at 540 nm. Xyloglucanase (2 μM) was incubated without (*filled square*) or with the inhibitor at 1 μM (*filled circle*) and 2 μM (*filled triangle*) and assayed at an increased concentration of xyloglucan (1–10 mg/ml) at 50 °C for 30 min. The reciprocal of substrate hydrolysis (*1/v*) for each inhibitor concentration was plotted against the reciprocal of the substrate concentration. The straight lines indicated the best fits for the data obtained by non-linear regression analysis and was analyzed by Lineweaver-Burk reciprocal equation. **b** Xyloglucanase (2 μM) was assayed using xyloglucan at 5 mg/ml (*filled circle*) and 10 mg/ml (*filled square*) with increasing concentrations of pepstatin A at 50 °C for 30 min. The reciprocal of substrate hydrolysis (*1/v*) was plotted against inhibitor concentration. The straight lines indicated the best fits for the data obtained by non-linear regression analysis and was analyzed by Dixon method

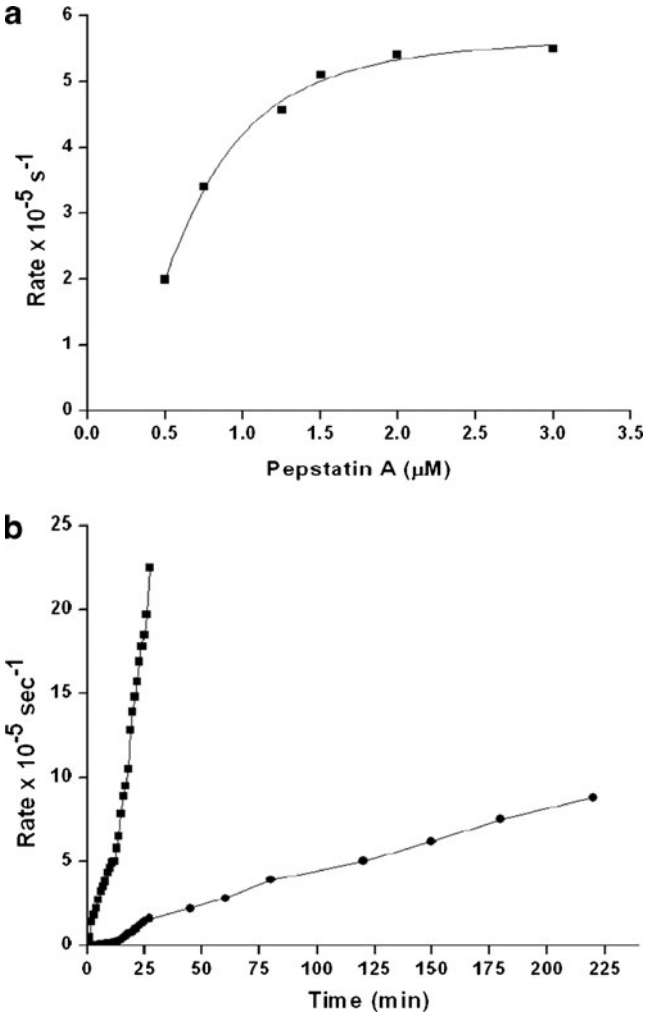

Fig. 3 **a** Dependence of xyloglucanase inhibition on pepstatin A concentration. The rate constants *k* was calculated from the progress curves recorded after the addition of xyloglucanase to the reaction mixture containing xyloglucan and pepstatin A. The solid line indicates the best fit of the data obtained. **b** Dissociation rate constant (k_6) for xyloglucanase-pepstatin A complex. Xyloglucanase (2 mM) was pre-incubated without (*filled square*) or with (*filled circle*) equimolar concentrations of pepstatin A for 120 min in sodium phosphate buffer, 0.05 M, pH 7.0. At the specified times indicated by the points, 5 μl of the preincubated sample was removed, diluted 5000-fold in the same buffer, and assayed for the xyloglucanolytic activity using xyloglucan (100 mg/ml). The rate constant associated with the regeneration of activity (k_6) was determined by estimating the reducing sugar as described under "Materials and Methods"

conditions, v_0 and the effective inhibitor concentration can be considered approximately equal to 0, and the rate of activity regeneration will provide the k_6 value. After pre-incubating xyloglucanase with pepstatin A, the enzyme inhibitor mixture was diluted 5000-fold into the assay mixture containing the substrate at 50 *Km*. By least-squares minimization of Eq. 2 to the data for recovery of enzymatic activity, the determined k_6 value was $2.85 \pm 1.2 \times 10^{-8} s^{-1}$ (Fig. 3b), which clearly indicated a very slow dissociation of *EI**. The final steady-state rate v_S was determined from the control that was pre-incubated without the inhibitor. The value of the rate constant k_5, associated with the isomerization of *EI* to *EI**, was $14.5 \pm 1.5 \times 10^{-5} s^{-1}$, as obtained from fits of Eq. 5 to the onset of inhibition data using the experimentally determined values of K_i and k_6 (Table 1). The

$$ES \xrightarrow{k_7} E + P$$

$$k_1 \uparrow\downarrow k_2$$

$$\text{a)} \quad E + I \underset{k_4}{\overset{k_3}{\rightleftharpoons}} EI$$

$$\text{b)} \quad E + I \underset{k_4}{\overset{k_3}{\rightleftharpoons}} EI \underset{k_6}{\overset{k_5}{\rightleftharpoons}} EI^*$$

$$\text{c)} \quad E \underset{k_{-cf}}{\overset{k_{cf}}{\rightleftharpoons}} E^* + I \underset{k_6}{\overset{k_5}{\rightleftharpoons}} EI^*$$

Scheme 1 The possible mechanisms for the slow-binding inhibition phenomenon E stands for free enzyme, I is free inhibitor, EI is a rapidly forming pre-equilibrium complex, and EI* is the final enzyme-inhibitor complex. E may undergo inter conversion into another form E*, which binds to the inhibitor by a fast step, where k_{cf} and k_{-cf} stand for the rate constants for forward and backward reaction respectively, for the conversion of the enzyme

overall inhibition constant K_i^* is a function of $k_6/(k_5+k_6)$ and is equal to the product of K_i and this function. The k_6 value indicated a slower rate of dissociation of *EI** complex and the half-life $t_{1/2}$, for the reactivation of EI* as determined from k_6 values was $62\pm1.8\times10^2$h, suggesting higher binding affinity of pepstatin A toward xyloglucanase.

Scheme 1 describes two alternative models for the time-dependent inhibition. The mechanism in Scheme 1a, where the binding of the inhibitor to the enzyme is slow and tight but occurs in a single step, is eliminated based on the data of Table 1. Scheme 1c represents the inhibition model where the inhibitor binds only to the free enzyme because the inhibitor has a measurable effect on the initial rates before the onset of slow tight binding inhibition, which has slowly adopted the transition-state configuration, can also be eliminated by the observed rates of onset of inhibition. Our foregoing results for the inactivation of xyloglucanase were, therefore, consistent with the slow-tight binding mechanism as described in Scheme 1b.

Table 1 Inhibition constants of pepstatin A against xyloglucanase

Inhibition constants	Values
IC_{50}	3.5±0.5 μM
K_i	1.25±0.5 μM
K_i^*	27±1 nM
k_5	$14.5\pm1.5\times10^{-5}$ s^{-1}
k_6	$2.85\pm1.2\times10^{-8}$ s^{-1}
$t_{1/2}$	$62\pm1.8\times10^2$h

Fluorescence Studies on Enzyme-Inhibitor Interactions

The kinetic analysis revealed a two-step inhibition mechanism, where the EI complex isomerizes to a tightly bound, slow dissociating EI* complex. This isomerization is a consequence of the conformational changes induced in xyloglucanase due to the binding of pepstatin. The localized conformational changes induced in xyloglucanase due to interactions with pepstatin were investigated by exploiting the intrinsic fluorescence by excitation of the π-π* transition in the Trp residues. The fluorescence emission spectra of xyloglucanase exhibited an emission maxima (λ_{max}) at 340 nm as a result of the radiative decay of the π-π* transition from the Trp residues, confirming the hydrophilic nature of the Trp environment (Fig. 4a). The titration of the native enzyme with increasing concentrations of pepstatin resulted in a concentration dependent quenching of the tryptophanyl fluorescence (Fig. 4a inset). However, the λ_{max} of the fluorescence profile indicated no blue or red shift, revealing that the ligand binding caused reduction in the intrinsic protein fluorescence. The subtle conformational changes induced during the isomerization of EI to EI* was monitored by analyzing the tryptophanyl fluorescence of the complexes as a function of time. Binding of pepstatin resulted in an exponential decay of the fluorescence intensity as indicated by a sharp decrease in the quantum yield of fluorescence followed by a slower decline to a stable value

Fig. 4 **a** Steady-state fluorescence emission spectra of xyloglucanase as a function of pepstatin A. Protein fluorescence was excited at 295 nm, and emission was monitored from 300 to 400 nm at 25 °C. Titration was performed by the addition of different concentrations of the inhibitor to a fixed concentration of enzyme. Xyloglucanase (2 μM) was dissolved in sodium phosphate buffer, 0.05 M, pH 7.0, and the concentrations of pepstatin A used were 0 μM (*filled square*), 0.70 μM (*filled circle*), 1.45 μM (*filled triangle*), 2.15 μM (*filled down-pointing triangle*), 3.5 μM (*filled left-pointing pointer*), 4.30 μM (*filled right-pointing pointer*), 5 μM (*empty square*), 5.82 μM (*empty circle*), 6.5 μM (*empty diamond*). The curve in the inset represents the best fit of the fluorescence quenching data of xyloglucanase at 342 nm (λ_{max}) as a function of pepstatin A concentration. **b** Time-dependent effect of pepstatin A on the fluorescence quenching of xyloglucanase. Pepstatin A was added to xyloglucanase (2 μM) at the specified time (indicated by the *arrow*), and the fluorescence emission was monitored for 300 s at a data acquisition time of 0.1 s. The excitation and emission wavelengths were fixed at 295 and 340 nm, respectively. The data were the average of eight scans with the correction for buffer and dilutions. The concentrations of pepstatin A used were 0 μM (*filled square*) and 1.5 μM (*filled circle*). **c** Effect of pepstatin A concentration on the tryptophan fluorescence of xyloglucanase. A specified concentration of xyloglucanase (2 μM) was treated with increasing concentrations of pepstatin A (0–7 μM). The fluorescence was measured at 25 °C (excitation 295 nm and emission 340 nm). Each measurement was repeated five times, and the average values of the fluorescence intensity at 340 nm were recorded. Control experiments with the buffer and inhibitor were performed under identical conditions. The fluorescence changes ($F-F_0$) were plotted against the inhibitor concentrations. The resulting hyperbola indicates the best fit of the data obtained

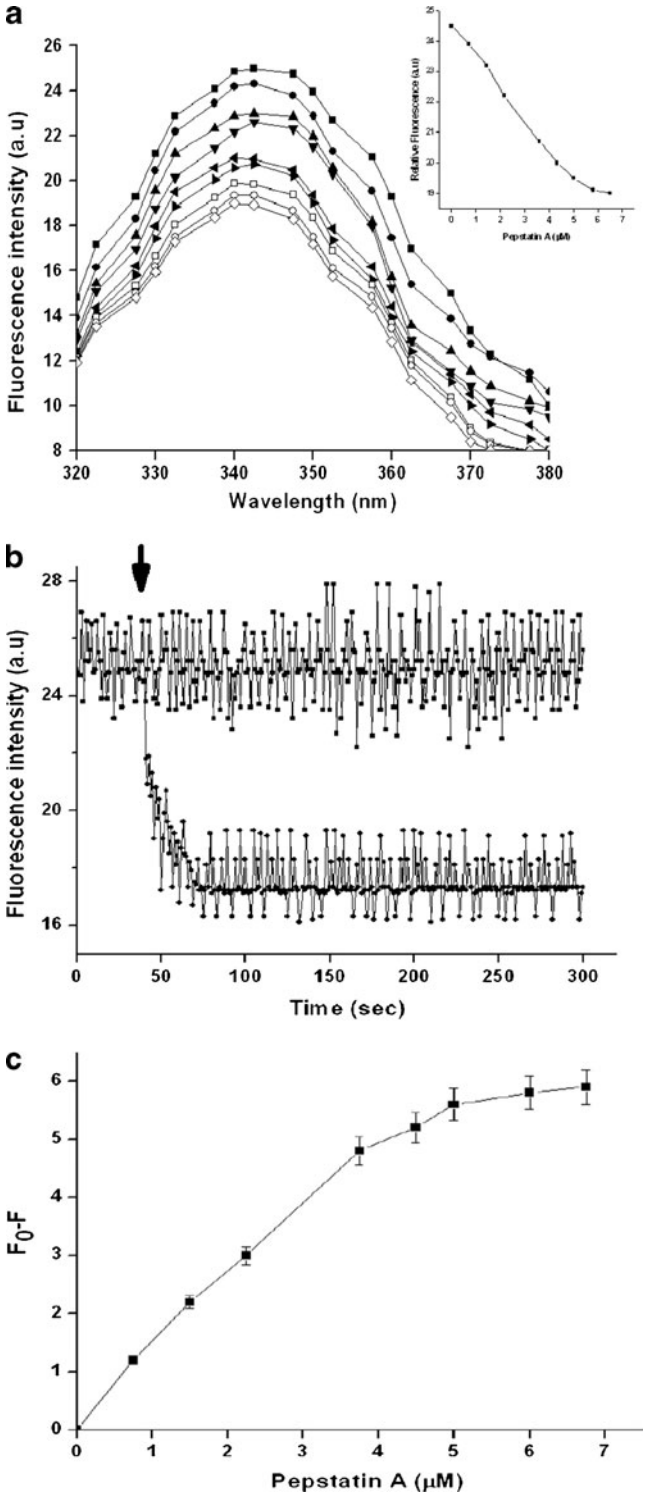

(Fig. 4b). Furthermore, the titration of pepstatin against xyloglucanase revealed that the magnitude of the initial rapid fluorescence loss (F_0-F) increased in a saturation-type manner (Fig. 4c), which corroborated the two-step slow-tight binding inhibition of the enzyme by the inhibitor. From the data in Fig. 4c, the magnitude of the rapid fluorescence decrease at a specific inhibitor concentration was found to be close to the total fluorescence quenching observed in Fig. 4a, indicating that the EI and EI* complexes have the same intrinsic fluorescence. The value of K_i determined by fitting the data for the magnitude of the rapid fluorescence decrease (F_0-F) was 1.25±0.75 μM and the k_5 value determined from the data derived from the slow decrease in fluorescence was $13.5\pm0.5\times10^{-5}\,s^{-1}$. These rate constants are in good agreement with that obtained from the kinetic analysis, therefore, the initial rapid fluorescence decrease can be correlated to the formation of the reversible complex EI, whereas the slow, time-dependent decrease reflected the accumulation of the tight bound slow dissociating complex EI*.

Effect of Pepstatin A on the Isoindole Fluorescence of Xyloglucanase by OPTA

The role of essential histidine and lysine residues in the active site of xyloglucanase were studied using chemical modification with 2,4,6-trinitrobenzenesulfonic acid (TNBS) and diethylpyrocarbonate (DEP). The involvement of these residues in the formation of an isoindole derivative was determined using chemoaffinity label OPTA (manuscript communicated). To investigate the binding of the inhibitor to the active site and changes in the native intermolecular interactions, the isoindole fluorescence of xyloglucanase was monitored (Fig. 5). The native enzyme did

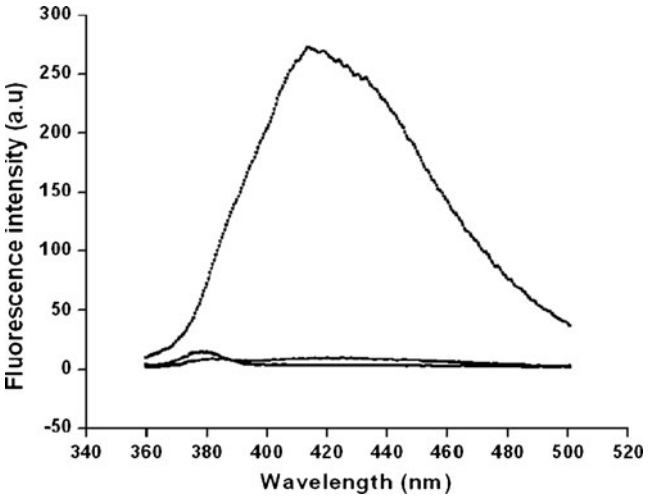

Fig. 5 Isoindole fluorescence of xyloglucanase on reaction with OPTA and pepstatin A. Xyloglucanase (2 μM) was treated without or with pepstatin A (2 μM) and incubated at 25 °C for 20 min and then further incubated with a fresh solution of OPTA (50 μM). The isoindole fluorescence of the xyloglucanase bound OPTA was measured with excitation at 330 nm. The lines represent the isoindole fluorescence of xyloglucanase (*filled circle*), xyloglucanase + OPTA (*filled square*), and xyloglucanase + pepstatin A (preincubated) and OPTA (*filled triangle*) and are the average of six scans with corrections from buffer and respective controls

not show fluorescence when excited at 338 nm, however on incubation with OPTA resulted in an increase in the fluorescence with a λ_{max} at 420 nm due to the formation of the isoindole derivative. The pepstatin-preincubated xyloglucanase failed to react with OPTA as revealed by the total loss of isoindole fluorescence, which not only confirmed the binding of the inhibitor to the active site of xyloglucanase but also further revealed that the binding of pepstatin resulted in the formation of a new set of hydrogen bonding and other non-ionic interactions. These altered weak interactions cause disruption of the native hydrogen bonding network of the histidine and lysine residues, which are essential for the formation of isoindole derivative.

Circular Dichroism Analysis of Enzyme-Substrate-Pepstatin A Complexes

To evaluate the effects of pepstatin A on the secondary structure of the enzyme, the CD spectra of xyloglucanase-inhibitor complex were analyzed. The estimated secondary structure contents from the CD analysis are 52 % α-helix, 28 % β-sheet, and 16 % aperiodic structure. The CD spectrum of the enzyme-pepstatin complex showed a pronounced shift in the negative band at 218 nm of the native enzyme to 224 nm revealing a subtle change in the secondary structure of the enzyme upon ligand binding (Fig. 6). A comparison of the changes in the secondary structure of xyloglucanase-pepstatin A complex with that of xyloglucanase-substrate complex was studied (data not shown). Interestingly, xyloglucanase-pepstatin A and xyloglucanase-substrate complexes exhibit a similar pattern of negative ellipticity in the far-UV region.

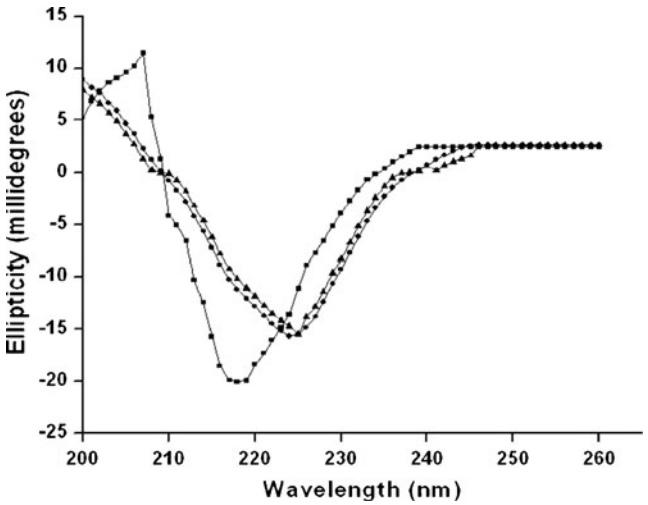

Fig. 6 Effect on the secondary structure of xyloglucanase upon binding of pepstatin A. Far-UV circular dichroism spectra of the unliganded xyloglucanase and its complexes with pepstatin and xyloglucan are shown. The xyloglucanase (50 nM) was dissolved (as described under "Materials and Methods") and CD spectra were recorded in the absence (*filled square*) or in the presence of pepstatin A at 5 μM (*filled circle*) and 10 μM (*filled triangle*) from 200 to 260 nm at 4 °C. Each spectrum represents the average of five scans

Discussion

A number of naturally occurring reversible glycosidase inhibitors such as nojirimycin, castanospermine, swainsonine, and acarbose have been reported [25]. Another class of inhibitors is the synthetic analogues of sugars containing reactive groups such as epoxides, isothiocyanates, α-halocarbonyls [25, 26], triazoles [27] and thiasugars [28]. There are reports of mechanism-based inhibitors such as conduritol epoxides, the quinone methide-generating glycosides, and the glycosylmethyl triazenes. A diverse array of extremely potent, basic, nitrogen-containing inhibitors has been developed over the years, and they have been found to be of great utility in the study of the glycosidase mechanism [25, 29]. These are more selective inhibitors whose efficacy depends upon binding and subsequent enzymatic action to generate a reactive species. Although a plethora of synthetic inhibitors has been reported, there is a lacuna of naturally occurring low molecular weight inhibitors of glycosidases from microorganisms. Pepsin and xyloglucanase catalyze hydrolytic cleavage of two different substrates made of peptide bond and glycosidic bond, respectively. Pepsin, a model enzyme for aspartic protease, did show any activity on xyloglucan, a sugar polymer made of glycosidic bond. Xyloglucanase did not show any activity against protein substrates, such as hemoglobin and casein, made of peptide bond (data are not shown), indicating these enzymes are absolutely specific toward their natural substrates.

The current work reports an aspartic protease inhibitor, pepstatin A, exhibiting slow-tight binding inhibition against xyloglucanase from *Thermomonospora* sp. There are several reports on the inhibition of pepstatin A against aspartic proteases [24], but this is the first study that explores the inhibition mechanism of this specific aspartic protease inhibitor against a xyloglucanase. The inhibitor showed exceptionally high potency against the thermostable xyloglucanase from *Thermomonospora* sp, and its 1:1 molar ratio of interaction with the enzyme indicated its "tight binding" nature. The two-step inhibition mechanism was corroborated by the equilibrium binding studies of the enzyme and inhibitor and the correlation of the kinetic data with the conformational changes induced in the enzyme-inhibitor complexes. The slow-binding inhibition of enzymes can be illustrated kinetically by three mechanisms as described in Scheme 1. Simple second-order interaction between the enzyme (E) and the inhibitor (I) could result in slow-binding inhibition where the rate of complex formation is slow. Kinetically, when an inhibitor has a low K_i value and the concentration of I varies in the region of K_i, both k_3I, and k_4 values would be low. These low rates of association

and dissociation would lead to slow-binding inhibition (Scheme 1a). Alternatively, binding may also involve two steps where there is a rapid formation of an initial collisional complex EI, that subsequently undergoes slow isomerization to form the final tight complex EI* (Scheme 1b). The extent of EI* formation depends on the affinity of the EI complex and the relative rates of formation of EI* and its relaxation to EI. Slow-binding inhibitor can also arise due to an initial slow inter conversion of the enzyme E into another form E* which binds the inhibitor by a fast step (Scheme 1c). Kinetically, these mechanisms can be differentiated by investigating the behavior of the enzyme-inhibitor system at varying concentrations of the inhibitor. Scheme 1a would predict that in the presence of substrate the initial rate of substrate hydrolysis will be independent of inhibitor concentrations as the concentration of EI would be significantly low. However, in Scheme 1b, the inhibitor will inhibit the enzyme competitively at the onset of the reaction, and at increasing concentration of inhibitor, the initial rate of substrate hydrolysis will decrease hyperbolically. The kinetic analysis of the xyloglucanase inhibition in this paper provides a unique opportunity for the quantitative determination of these rates and affinities, which can be extended to other slow-tight binding inhibition reactions. The formation of EI complex between xyloglucanase and pepstatin A was too rapid to be measured at steady-state kinetics and was likely to be near diffusion control. However, the isomerization of EI to the second tightly bound enzyme-inhibitor complex, E^*, was too slow and relatively independent of the stability of the EI or the ability of the inhibitor to stabilize the EI^*. The k_6 values revealed very slow dissociation of the inhibitor from the EI^*, indicating a highly stable, non-dissociative nature of the second complex. Therefore, for slow-tight binding inhibition the major variable is k_6, the first-order rate constant associated with the conversion of EI^* to EI, and the apparent inhibitor constant K_i^* depends on the ability of the inhibitor to stabilize the EI^*. The half-life as derived from the k_6 value indicated a longer half-life of the EI^*, which is an essential parameter for an inhibitor to have biomedical applications.

The characteristic feature of slow binding inhibition is the induction of conformational changes in the enzyme-inhibitor complex, resulting in the clamping down of the enzyme to the inhibitor, thus the formation of a stable enzyme-inhibitor complex. The two-step inhibition mechanism of xyloglucanase by pepstatin A was reflected in the quenching pattern of the fluorescence of the enzyme-inhibitor complexes. The tryptophanyl fluorescence appears to be uniquely sensitive to shielding by a variety of ligands because of the propensity of the excited indole nucleus to emit energy in the excited state. We have exploited the Trp residues of xyloglucanase to investigate the localized conformational changes induced upon substrate or pepstatin binding. Our foregoing results have suggested that pepstatin binds in the active site of the enzyme and is a unique example where the conformational changes were investigated by monitoring the radiative decay of the π-π* transition from the Trp residues. The fluorescence quenching of xyloglucanase by pepstatin revealed that the binding of pepstatin reduces the quantum yield of the Trp emission. These results were further corroborated by the quenching studies of xyloglucanase in the presence of the substrate. The comparison of the emission spectra of xyloglucanase upon binding of pepstatin with that of the substrate led us to conclude that the inhibitor binds to the active site of the enzyme. The concentration-dependent quenching of Trp fluorescence showed that λ_{max} did not undergo any red or blue shift, wherein the quenching of fluorescence was considerably high. These findings indicated that the polarity of the Trp environment was negligibly altered after binding of the inhibitor, suggesting minimal conformational changes in the tertiary structure of the xyloglucanase. The rate constants derived from the fluorescence analysis of the complexes reinforced the values derived from the kinetic analysis. Therefore, we propose that the initial rapid fluorescence loss reflected the formation of the reversible complex EI, whereas the subsequent slower decrease was correlated to the accumulation of the tightly bound complex EI*. Any disturbance in the environment of tryptophan residues may be reflected in an alternation in emission wavelength, quantum yield, and susceptibility to quenching [30]. Energy transfer to an acceptor molecule having an overlapping absorption spectrum can also contribute to fluorescence quenching [31]. However, because the inhibitor has no absorption in the region of 290–450 nm, the fluorescence quenching due to the energy transfer between pepstatin and the tryptophan residues of xyloglucanase have been neglected. The other possibility is the presence of multiple sites, where binding at one induced rapid fluorescence change and at a second site caused the slow fluorescence decrease. This was verified by titrating a fixed concentration of xyloglucanase with increasing concentrations of pepstatin. The xyloglucanolytic activity decreased linearly with increasing concentrations of pepstatin yielding a stoichiometry close to 1:1 (also revealed by fluorescence) expected for the slow-tight binding inhibition, therefore inconsistent with the presence of multiple high affinity sites. From the physical explanation for the quenching process, it was apparent that the pepstatin induced fluorescence quenching followed the formation of both the complexes. The agreement of the rate constants concomitant with the fluorescence changes observed during the time-dependent inhibition led us to correlate the localized conformational changes in the enzyme-inhibitor complex to the isomerization of the EI to EI*. Our interpretation for the changes observed in the secondary structure of xyloglucanase due to the binding of the substrate to the active site can be correlated to the similar

pattern of changes observed due to the binding of pepstatin A. Thus, we have concluded from the fluorescence and CD studies, that pepstatin A binds to the active site of xyloglucanase and causes inactivation.

Conformational integrity of the active site of an enzyme is essential for its catalysis, and investigations on the molecular orientation of the functional groups of the active site as well as their microenvironment are areas of growing scientific interest. Chemo-affinity labeling is a powerful technique to assign the binding sites of ligand-macromolecule complexes, which combines some of the advantages of both the photoactivated and electrophilic affinity labeling [32]. OPTA is a bifunctional, fluorescent chemoaffinity label, which until recently was known to have absolute specificity for amino and thiol groups [33] for the formation of an isoindole derivative. However, application of OPTA as a probe to ascertain the conformational flexibility and polarity of the active site of xyloglucanase by the formation of a fluorescent isoindole derivative with the lysine and histidine residue is elucidated in our laboratory (manuscript communicated). OPTA contains two aldehyde groups, one of which reacts with the primary amine of lysine while the second group reacts with the secondary amine of the imidazole ring of histidine, resulting in the formation of the isoindole derivative. Our foregoing results revealed that, when xyloglucanase was preincubated with pepstatin A, OPTA failed to form the isoindole derivative, as reflected by the loss of fluorescence. The inability of OPTA to form the isoindole derivative with the pepstatin A-bound xyloglucanase could be attributed to the interaction of the inhibitor with either lysine or histidine or both the residues, thereby changing the native molecular interactions of these residues. The chemical structure of pepstatin is isovaleryl-L-valyl-L-valyl-statyl-L-alanyl-statin, which contains two residues of unusual amino acid statin ((3S,4S)-4- amino-3-hydroxy-6-methyl-heptanoic acid). The statin is the major structural component responsible for the pepstatin inhibition against the aspartic protease. Aspartic proteases consist of two carboxyl groups at the active site, one of which has to be protonated and the other deprotonated for the enzyme to be active. Aspartic protease undergoes a general acid–base catalysis that may be called a "push-pull" mechanism. The nucleophilic attack is achieved by two simultaneous proton transfers, one from a water molecule to the diad of the two carboxyl groups and a second one from the diad to the carbonyl oxygen of the substrate with the concurrent CO-NH bond cleavage. Pepstatin is an analog of the transition state of peptic catalysis that tightly binds to active site of the enzyme [34]. In the case of xyloglucanase the active site contains two essential catalytic groups, one playing the role of acid/base and the other functioning as a nucleophile. We propose that pepstatin makes several interactions with the active site residues of xyloglucanase both through hydrogen bonds and non-bonded interactions. Based on the existing experimental evidences, we further propose that the other residues of the inhibitor could form many intermolecular hydrogen bonds and other weak interactions with the residues in or near the active site of xyloglucanase. We also visualize that the tight binding nature of pepstatin A in conjunction with the multiple nonbonded interactions may be sufficient to interfere in the native weak interactions between the carboxyl groups, the lytic water molecule, and the essential histidine residue of the active site, leading toward the inactivation of xyloglucanase.

Conclusion

Based on our observations, we conclude that the inhibition of xyloglucanase by pepstatin A followed slow-tight binding inhibition mechanism and the induced conformational changes are conveniently monitored by near and far UV analysis. Chemo-affinity labeling of the enzyme active site has demonstrated that the inactivation of xyloglucanase is due to the interference in the electronic microenvironment and disruption of the hydrogen bonding network between the essential histidine and other residues involved in catalysis. However, the crystal structure of the enzyme-inhibitor complex will aid to understand the mechanism of inactivation of xyloglucanse in depth and will further shed light on the molecular interactions between the enzyme and inhibitor.

Acknowledgments MR and VM acknowledge the financial support and the senior research fellowship from CSIR Emeritus Scheme, Govt. of India respectively. MR is thankful to Dr Barry McCleary, Megazyme International Ireland Ltd for xyloglucan from tamarind seeds.

References

1. Gloster TM, Ibatullin FM, Macauley K, Eklo JM, Roberts S et al (2007) Characterization and three-dimensional structures of two distinct bacterial xyloglucanases from families GH5 and GH12*. J Biol Chem 282:19177–19189
2. Martinez-Fleites C, Guerreiro CIPD, Baumann MJ, Taylor EJ et al (2006) Crystal structures of *Clostridium thermocellum* xyloglucanases, XGH74A, reveal the structural basis for xyloglucan recognition and degradation. J Biol Chem 281:24922–24933
3. Benko Z, Siika-aho M, Viikari L, Reczey K (2008) Evaluation of role of xyloglucanase in the enzymatic hydrolysis of lignocellulosic substrates. Enzym Microb Technol 43:109–114
4. Menon V, Prakash G, Rao M (2010) Enzymatic hydrolysis and ethanol production using xyloglucanase and *debaryomyces hansenii* from tamarind kernel powder: galactoxyloglucan predominant hemicelluloses. J Biotechnol 148:233–239
5. Wong DDWS, Chan VJ, McCormack AA, Batt SB (2010) A novel xyloglucan- specific endo-β-1,4- glucanase: biochemical properties and inhibition studies. Appl Microbiol Biotechnol 86:1463–1471

6. Sørensen JF, Kragh KM, Sibbesen O, Delcour J, Goesaert H, Svensson et al (2004) Potential role of glycosidase inhibitors in industrial biotechnological applications. Biochim Biophys Acta 1696:275–287
7. York WS, Qin Q, Rose JK (2004) Proteinaceous inhibitors of endo-beta-glucanases. Biochim Biophys Acta 1696:223–233
8. Hanada K, Nishiuchi Y, Hirano H (2003) Amino acid residues on the surface of soybean 4-kDa peptide involved in the interaction with its binding protein. Eur J Biochem 270:2583–2592
9. Scarafoni A, Ronchi A, Duranti M (2010) gamma- Conglutin, the Lupinus albus XEGIP-like protein, whose expression is elicited by chitosan, lacks the typical inhibitory activity against GH12 endo-glucanases. Phytochemistry 71:142–148
10. Yoshizawa T, Shimizu T, Yamabe M, Taichi M, Nishiuchi Y, Shichijo N et al (2011) Crystal structure of basic 7S globulin, a xyloglucanspecific endo-β-1,4-glucanase inhibitor protein-like protein from soybean lacking inhibitory activity against endo-β-glucanase. FEBS J 278:1944–1954
11. Yoshizawa T, Shimizu T, Hirano H, Sato M, Hashimoto H (2012) Structural basis for the inhibition of xyloglucan-specific endo-β-1,4-glucanase (XEG) by XEG-protein inhibitor. J Biol Chem. doi:10.1074/jbc.M112.350520
12. Umezawa H, Aoyagi T, Morishima H, Hamed M, Takeuchi T (1970) Pepstatin, a new pepsin inhibitor produced by Actinomycetes. J Antibiot 23:259–262
13. Eder J, Hommel U, Cumin F, Martoglio B, Gerhartz B (2007) Aspartic proteases in drug discovery. Curr Pharm Des 13:271–285
14. Dash C, Kulkarni A, Dunn B, Rao M (2003) Aspartic protease inhibitors: implications in drug development. Crit Rev Biochem Mol 38:89–119
15. Nguyen J-T, Hamada Y, Kimura T, Kiso Y (2008) Design of potent aspartic protease inhibitors to treat various diseases. Arch Pharm Chem Life Sci 341:523–535
16. Vinod V, Rao M (2004) Slow tight binding inhibition of xylanase by an aspartic protease inhibitor. J Biol Chem 279:47024–47033
17. Pol D, Menon V, Rao M (2012) Biochemical characterization of a novel thermostable xyloglucanase from an alkalothermophilic *Thermomonospora* sp. Extremophiles 16:135–146
18. Mandels M, Weber J (1969) The production of cellulases. Adv Chem 95:391–414
19. Lowry F, Rosebrough NJ, Farr AL, Randall RJ (1951) Protein measurement with the folin phenol reagent. J Biol Chem 193:265–275
20. Dixon M (1953) Determination of enzyme-inhibitor constants. Biochem J 55:170–171
21. Cleland WW (1979) The kinetics of enzyme catalyzed reactions with two or more substrates or products—II: inhibition, nomenclature and theory. Biochim Biophys Acta 67:173–187
22. Morrison JF, Walsh CT (1988) The behaviour and significance of slow-binding inhibitors. Adv Enzymol Relat Areas Mol Biol 61:201–302
23. Lakowicz JR (1983) Principles of fluorescence spectroscopy. Plenum, NY
24. Rich DH, Bernatowicz MS, Agarwal NS, Kawai M, Salituro FG, Schmidt PG (1985) Inhibition of aspartic proteases by pepstatin and 3-methylstatine derivatives of pepstatin. Evidence for collected-substrate enzyme inhibition. Biochemistry 24:3165–3173
25. Legler G (1990) Glycoside hydrolases: mechanistic information from studies with reversible and irreversible inhibitors. Adv Carbohydr Chem Biochem 48:319–385
26. Withers SG, Aebersold R (1995) Approaches to labeling and identification of active site residues in glycosidases. Protein Sci 4:361–372
27. Rossi LL, Basu A (2005) Glycosidase inhibition by 1-glycosyl-4-phenyl triazoles. Bioorg Med Chem Lett 15:3596–3599
28. Yuasa H, Izumi M, Hashimoto H (2009) Thiasugars: potential glycosidase inhibitors. Curr Top Med Chem 9:76–86
29. Stutz AE (1999) Immunosugars as glycosidase inhibitors: nojirimycin and beyond. Wiley, Weinheim, pp 95–120
30. Pawagi AB, Deber CM (1990) Ligand-dependent quenching of tryptophan fluorescence in human erythrocyte hexose transport protein. Biochemistry 20:950–955
31. Cheung HC (1991) Topics in fluorescence spectroscopy. In: Lakowicz JR (ed) Principles, vol 2. Plenum, New York, pp 127–176
32. Simons SS Jr, Johnson DF (1978) Reaction of o-phthalaldehyde and thiols with primary amines: fluorescence properties of 1-alkyl (and aryl) thio-2-alkylisoindoles. Anal Biochem 90:705–725
33. Palczewski K, Hargrave PA, Kochman M (1983) o-phthalaldehyde, a fluorescence probe of aldolase active site. Eur J Biochem 137:429–435
34. Marciniszyn J, Hartsuck JA, Tang J (1976) Mode of inhibition of acid proteases by pepstatin. J Biol Chem 251:7088–7709